# Darpa Denizalti Modelinde Derinliğe Bağlı Olarak Değişen Hidrodinamik Manevra Türevlerinin ve Yatay Stabilitenin İncelenmesi

**Furkan Çavdar [1], Şakir Bal [2]**

[1,2] Gemi İnşaatı ve Deniz Bilimleri Fakültesi, İstanbul Teknik Üniversitesi,
Ayazaga Kampüsü, Maslak-Sariyer, İstanbul, Türkiye

[1] (sorumlu yazar), cavdarf@itu.edu.tr, ORCID: 0000-0003-3245-5432
[2] sbal@itu.edu.tr, 0000-0001-8688-8482

## ÖZET

Bilindiği üzere, DARPA SUBOFF denizaltı modeli derin suda yatay stabiliteye sahip değildir. Bu çalışmada, denizaltı modelinin periskop (şnorkel) seyri esnasında veya su yüzeyine yakın hareket ederken yatay stabilitesi 3 serbestlik dereceli olarak tespit edilmiştir. Denizaltı stabilitesi ve hidrodinamik manevra türevleri tespit edilirken farklı derinliklerde yanal öteleme kuvvetine ait doğrusal katsayılar ve savrulma açısal momentine ait doğrusal katsayılar kullanılmıştır. Denizaltı çapı D olmak üzere, derinlikler 1.1D, 2.2D, 3.3D ve 6D olarak seçilmiştir. Manevra türevleri hesaplamalı akışkanlar dinamiği metodlarıyla bir seri sistematik analiz yapılarak elde edilmiştir. Hesaplamalı analizlerde gerekli doğrulama çalışmaları da yapılmıştır. Hesaplamalı akışkanlar dinamiği analizlerinde boyuna ve yanal kuvvet türevleri, ve savrulma momenti türevleri hesaplanarak doğrusal modelde $X0$, $Xv$, $Xd$, $X_\delta$, $Yv$, $Yr$, $Y_\delta$. $Nv$, $Nr$ ve $N_\delta$ katsayıları belirlenmiş ve hidrodinamik model oluşturulmuştur. Farklı derinliklere göre elde edilen hidrodinamik türevler ile denizaltının yatay stabiliteye sahip olup olmadığı tespit edilmiştir. Denizaltı modelinin, serbest su yüzeyine yakın seyir durumlarında yatay stabiliyete sahip olduğu ve 4.6D derinlikten itibaren ise yatay stabilitesini kaybettiği bulunmuştur.

**Anahtar kelimeler:** DARPA denizaltı modeli, yatay stabilite, manevra türevleri, HAD, derinlik etkisi.

**Makale geçmişi:** Geliş 08/03/2022 – Kabul 25/05/2022

https://doi.org/10.54926/gdt. 1084413

# An Investigation of Hydrodynamic Maneuvering Derivatives and Horizontal Stability of Darpa Suboff Depending on Depth

**Furkan Çavdar [1], Şakir Bal [2]**

[1,2] Istanbul Technical University Deptartment of Naval Architecture and Marine Engineering, Ayazaga Campus, Maslak-Sariyer, Istanbul

[1](corresponding author), cavdarf@itu.edu.tr, ORCID: 0000-0003-3245-5432
[2] sbal@itu.edu.tr, 0000-0001-8688-8482

## ABSTRACT

It is known that DARPA SUBOFF submarine model does not have a horizontal stability in deep water. In this study, the horizontal stability of submarine model moving during the periscope (snorkel) position or close to the free water surface, has been determined in 3 DoF (degrees of freedom). While determining the submarine stability and hydrodynamic maneuvering derivatives, linear coefficients of lateral translational force at different depths and linear coefficients of yaw angular moment were used. The depths were selected as 1.1D, 2.2D, 3.3D and 6D, here D is submarine diameter. The maneuvering derivatives were obtained by performing systematic analyzes with the computational fluid dynamics method. Necessary validation studies were also carried out in computational analyzes. In computational fluid dynamics analysis, longitudinal and lateral force derivatives, and yaw moment derivatives were determined and X0, Xv, Xd, $X_\delta$, Yv, Yr, $Y_\delta$, Nv, Nr ve $N_\delta$ terms were computed in the linear model. A hydrodynamic model was generated with these coefficients. The horizontal stability was then determined with the effects of different depths by using this hydrodynamic model. It has been found that the submarine model has horizontal stability when cruising close to the free water surface and loses its horizontal stability for water depths greater than 4.6D.

**Nomenclarute**

| | |
|---|---|
| C2 : | Hull, Sail and Stern Obsession Model |
| C4 : | Hull and Sail Obsession Model |
| CAD : | Computer Aided Drawing |
| D : | DARPA submarine diameter |
| DARPA : | The Defense Advanced Research Projects Agency |
| DSM : | DARPA Suboff Model |
| DTRC : | David Taylor Research Center |
| Gh : | Number of horizontal stability |
| Gv : | Number of vertical stability |
| HAD : | Computational Fluid Dynamics |
| I: | DARPA submarine yaw moment of inertia |
| L : | DARPA submarine model size |
| LES : | Big Eddy Simulations |
| m : | mass of DARPA submarine |
| N : | Submarine understeer moment component |
| Nv : | First-order derivative coefficient of moment N with respect to velocity v |
| Nr : | First-order derivative coefficient of moment N with respect to yaw speed r |
| $N_\delta$ : | N moment effect coefficient of rudder moment |
| PMM : | Planar Motion Mechanism |
| r : | Submarine yaw angular velocity |
| RANS : | Reynold Mean Navier Strokes Equations |
| u : | Submarine longitudinal velocity |
| v : | Submarine lateral velocity |

| | |
|---|---|
| VOF : | Volume Free Surface Modeling Method |
| X : | Submarine longitudinal force component |
| X0 : | Submarine resistance coefficient in the X plane |
| Xd : | The depth effect coefficient in the X plane |
| Xg : | Longitudinal center of gravity |
| $X_\delta$ : | Coefficient of rudder force in the X plane |
| Xv : | First-order derivative coefficient of X force with respect to v velocity |
| Y : | Submarine lateral force component |
| Yv : | First order derivative coefficient of Y force with respect to v velocity |
| Yr : | First-order derivative coefficient of Y force according to yaw speed r |
| $Y_\delta$ : | Coefficient of rudder force in the Y plane |
| ρ : | Sea density |

## 1. Introduction

Submarines moving close to the free surface are needed for reasons such as air requirement, battery charging, GPS location determination and communication with the base (Kırıkbaş et al., 2021a). Because of these needs, it is necessary to examine the course keeping capabilities and stability of submarines operating at different depths, including near surface. The course keeping capabilities and stability of submarines are directly dependent on many factors such as fin configuration, submarine form, rudders and the depth of the submarine from the free surface. Cruising stability in the horizontal plane can be determined by submarine hydrodynamic derivatives (coefficients). For this reason, the correct calculation of the hydrodynamic derivatives of submarines operating at different depths is important in the maneuver of submarines (Amiri et al., 2019).

In order to investigate the maneuvering performance of submarines, whether in deep water or near free surface, the determination of hydrodynamic derivatives is required. Generally, the methods used to determine the hydrodynamic derivatives of submarines were described as empirical methods, experimental methods and CFD methods. There are studies in the literature that describe the advantages and disadvantages of these methods compared to each other, and studies that examine these three working methods according to each other and share the maneuver results (ITTC, 2008). Also, there are studies in the literature that obtain hydrodynamic derivatives with CFD and empirical approaches and the derivatives are validated by experimental data (Duman, S., Bal, S., 2019). In order to develop these methods, some submarine models have been created to be used in the literature. There are studies in which the submarine models used in the common literature are introduced and standard maneuvering tests are applied (Kirikbas et al., 2021b). Darpa submarine model is an example of this. With the increase in the use of submarines, some regulations have been made to determine the maneuvering performance of submarines (Kirikbas et al., 2021c). Maneuver tests were also applied to the Darpa SUBOFF submarine model at different depths and at different drift angles, according to the standards determined, and the coefficients for the model were given for depths close to the surface (Efremov and Milanov, 2019). These linear coefficients are also evident for deep waters (Roddy 1990). In this study, it was reported that the submarine did not have horizontal stability in deep water conditions. The reason why DARPA Suboff Geometry does not have horizontal stability has been explained in the literature. It has been noted that for DARPA geometry, sail-induced and rudder-induced eddies are too large and quickly render the submarine model physically unstable (Ashok and Smith 2013). First of all, the stability of the system should be checked and only then will the hydrodynamic derivative determination work be meaningful. Therefore, in this study, a study was conducted on the calculation of derivatives after controlling the stability of the submarine at different depths (Racine and Peterson, 2012). So, what is the deep-water limit? It has been found that depth has a significant effect on submarine resistance when the depth Froude number is greater than 0.7 (Dogrul, A., 2019). Here, this depth limit has been chosen to define the deep-water case.

In this study, the STAR-CCM+ package program has been used to implement the CFD method. In the study, static drift tests were applied to determine the hydrodynamic derivatives representing the lateral velocity derivatives in accordance with the examples given in the literature. In addition, pure yaw tests were applied to determine the hydrodynamic derivatives representing the yaw angular velocity derivatives (Yoon, H., 2009). the wave resistance of submarine and rudder performance at different depths close to the free water surface were investigated. First, the results from CFD analysis were validated with those of experiments given in literature. Then, the hydrodynamic derivatives and rudder geometries derivatives were calculated on the horizontal axis for the DSM. The near-surface (snorkel) depths of the DSM have also been considered. According to these derivatives, the horizontal

stability characteristic of DSM, which is known as unstabile in deep water, at depths close to the free surface has been investigated.

## 2. Hydrodynamic Model

In this study, horizontal stability has been examined. The necessary quantities for investigating the horizontal stability are the lateral forces and yaw moment. Therefore, the model has three degrees of freedom. Three degrees of freedom are represented by two translational and one rotational motion. The force - moment symbols for these degrees of freedom are defined in Table 1 with the translation - rotational speeds and position - angle information.

**Table 1:** Symbols used for degrees of freedom of submarine.

| Degrees of Freedom | Remark | Force and moment | Translational and rotational speed | Position and Angle |
|---|---|---|---|---|
| 1 | X direction translation | X | u | x |
| 2 | Y direction translation | Y | v | y |
| 3 | N direction rotation | N | r | ψ |

The directions of translational and rotational motions are defined in Figure 1 with the arrow direction denoting the positive direction.
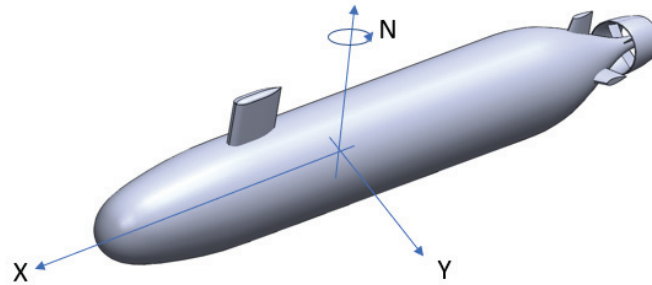


**Figure 1.** Three degrees of freedom system for submarine

The hydrodynamic model to be used in the three-degree-of-freedom system is given in equations 1, 2, and 3 as follows (Inoune et al., 1981);

$$X_H = X_o + X_v * v^2 + X_\delta * \delta^2 + X_d \tag{1}$$

$$Y_H = Y_v * v + Y_r * r + Y_\delta * \delta \tag{2}$$

$$N_H = N_v * v + N_r * r + N_\delta * \delta \tag{3}$$

Here, $X_H$ denotes the hydrodynamic forces in the X direction and $Y_H$ in the Y direction. $N_H$ represents the hydrodynamic moment in the N direction. The $X_o$ coefficient is the sum of the drag forces in the X direction obtained from the linear motion of the DSM while moving at a speed of 6.5 knots in deep

water without any rudder effect or drift effect. The $X_v$ coefficient represents the first-order derivative of the forces in the X direction according to the lateral velocity v. $X_d$ refers to the force acting in the x direction depending on the depth. The $X_\delta$ coefficient represents the sum of the rudder-induced forces in the x direction. The $Y_v$ coefficient represents the first-order derivative of the forces in the Y direction according to the v lateral velocity. The $Y_r$ coefficient represents the first orderr derivative according to the yaw angular velocity r of the forces in the Y direction, and the $Y_\delta$ coefficient represents the sum of the rudder-induced forces in the Y direction. The $N_v$ coefficient shows the first order derivative of the moments in the N direction according to the v lateral velocity, and the $N_r$ coefficient shows the first order derivative of the moments in the N direction according to the yaw angular velocity r. The $N_\delta$ coefficient is the sum of the rudder-induced moments in the N direction. All coefficients vary with depth, except for $X_o$. The submarine model image is shown in Figure 2. The physical variables and terms used for nondimensionalization are given Table 1.



**Figure 2.** DARPA Suboff 3D model

The non-dimensional terms used in the study are given in Table 2.

**Table 2.** Non-dimensionalization terms

| Variables | Terms for Nondimensionalization |
|---|---|
| Velocity | U |
| Angular velocity | U/L |
| Forces | $0.5*\rho*L^2*U^2$ |
| Moments | $0.5*\rho*L^3*U^2$ |
| Acceleration | $U^2/L$ |
| Angular acceleration | $U^2/L^2$ |

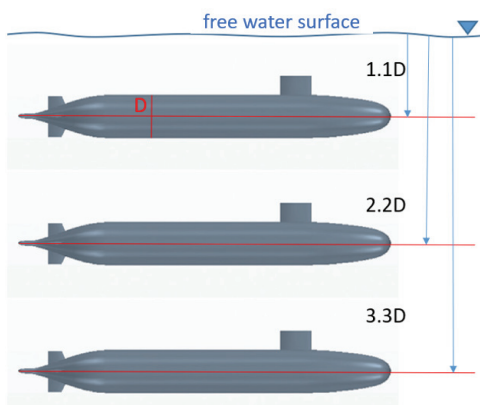In Figure 3, a submarine image at different depths is given.



**Figure 3.** DARPA Suboff at different depths

## 3. Validation and Verification Analysis

In order to minimize the effects of the outer boundaries on the computational domain, a sufficiently large computational domain should be selected. In this study, the main dimensions of the domain are 1.5L from the front, 5L from the back, 2L from the sides and 2L from the top and bottom (Sezen et al., 2018).

Three different mesh studies were performed for each model. The total number of meshes in the mesh structure and the increase in the mesh structure from coarse to fine show proportionality. There are studies in the literature with an increase rate of 1.6 mesh (Li et al., 2019). In this study, the mesh growth rate was chosen as 1.6. The mesh independence information and parameters are shown in Table 3.

**Table 3.** A study on mesh independence

| Depth | Naming | Basic size | Number of cells | Cell increase rate |
|---|---|---|---|---|
| 1.1D | Coarse | 10.00 | 727044 | - |
| 1.1D | Medium | 7.50 | 1223770 | 1.683 |
| 1.1D | Fine | 6.0 | 1927698 | 1.575 |
| 2.2D | Coarse | 10.0 | 677568 | - |
| 2.2D | Medium | 7.50 | 1115281 | 1.646 |
| 2.2D | Fine | 6.0 | 1766403 | 1.583 |
| 3.3D | Coarse | 10.0 | 662324 | - |
| 3.3D | Medium | 7.50 | 1086891 | 1.641 |
| 3.3D | Fine | 6.0 | 1738435 | 1.599 |
| Deep water | Coarse | 10.0 | 560894 | - |
| Deep water | Medium | 7.50 | 896523 | 1.598 |
| Deep water | Fine | 6.0 | 1408255 | 1.570 |

The results of static drift tests with $k - \varepsilon$ turbulence model at different depths are compared in Table 4. Thus, it has been noticed that the error level has decreased below 2 percent in X force, 4 percent Y force, and 3 percent N moment between the medium density mesh and fine mesh.

**Table 4.** Mesh percent difference values

| Depth | Mesh naming (difference) | %X difference | %Y difference | %N difference |
|---|---|---|---|---|
| 1.1D | Coarse-Medium | 0.58 | 3.30 | 3.72 |
| 1.1D | Medium-Fine | 0.07 | 3.02 | 2.55 |
| 2.2D | Coarse-Medium | 1.14 | 3.53 | 2.77 |
| 2.2D | Medium- Fine | 0.38 | 1.63 | 1.44 |
| 3.3D | Coarse-Medium | 0.99 | 2.59 | 0.70 |
| 3.3D | Medium- Fine | 0.01 | 1.21 | 0.78 |
| Deep Water | Coarse-Medium | 0.83 | 1.23 | 0.78 |
| Deep Water | Medium-Fine | 0.22 | 0.56 | 0.73 |

The mesh structure at 1.1D is shown in Figure 4. In order to accurately model the viscous effects of the submarine, a more fine mesh structure was created in the nose, sail and stern areas. In addition, in order to better model the effect of fluctuations on the free water surface, the mesh structure is

arranged according to the depth. This free water surface layer will allow the VOF solution to converge. The Y+ value should be between 30 and 300 in the analyzes to be made with the RANS method (Sezen et al., 2018; Duman and Bal, 2021). In this study, Y+ was chosen as 50. The boundary layer thickness in the mesh structure was calculated as 0.06 meters and modeled with 15 layers. The boundry layer expansion ratio was determined as 1.2. Time step in the analysis is chosen 0.2 sec.
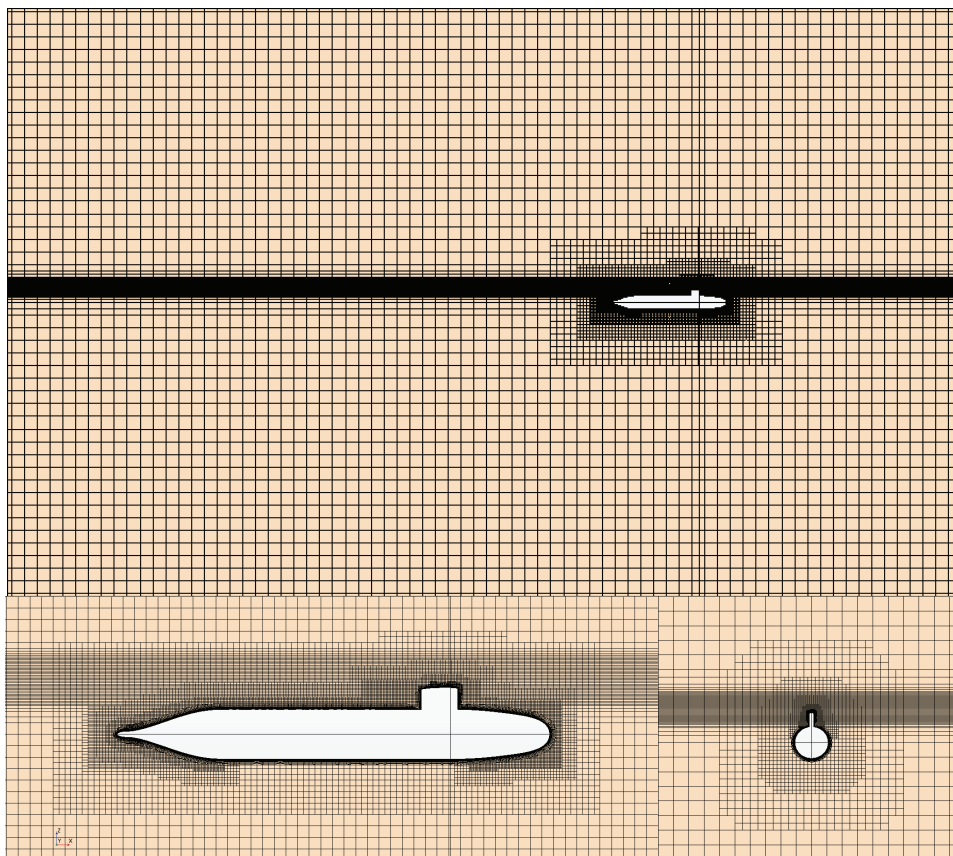


**Figure 4.** 1.1D mesh structure and computation domain

The flow around underwater platforms is turbulent, and a turbulence model should be chosen in accordance with the effects of Reynolds stresses in CFD studies using the RANS method. It has been observed that the "Realizable" $k - \varepsilon$ model responds better to dynamic tests both in terms of results and time optimization (Sakaki and Kerdabadi, 2020). Again, by comparing $k - \varepsilon$ and $k - \omega$ models in the literature, it is noted that the $k - \varepsilon$ model expresses the rotation effects better (Ray et al., 2009) as well as in non-dynamic tests in submarine maneuvering studies. In this study, $k - \varepsilon$ turbulence model was used in static drift tests, and realizable $k - \varepsilon$ turbulence model was applied in pure yaw tests.

Deep water validation data for different drift angles with respect to X, Y and N axes are given in Table 5. While the forces and moments were obtained in the analysis results, the forces and moments in the X force, Y force and N moment were used in the analyses. The forces and moment obtained as a result of the analyses are nondimensional according to the terms given in Table 1. As expected, the numbers are negative on the X axis and change the sign on the Y and N axes according to the direction of the drift angle. In the present CFD analysis, Darpa Submarine is assumed to be axisymmetrical and the analysis results show symetrical behaviors. Therefore, validation data (Roddy, 1990) and analysis results by CFD actually produced different errors under the same conditions. Experimental data do not show symmetrical results.

**Table 5.** Validation in deep water case (Roddy, 1990)

| Drift angle | X nondimensional force | | |
| --- | --- | --- | --- |
| | Validation Data | Analysis Result | %Error |
| -4 | $-1.13*10^{-3}$ | $-1.15*10^{-3}$ | 1.2 |
| -2 | $-1.16*10^{-3}$ | $-1.08*10^{-3}$ | 6.3 |
| 2 | $-1.15*10^{-3}$ | $-1.08*10^{-3}$ | 6.0 |
| 4 | $-1.13*10^{-3}$ | $-1.15*10^{-3}$ | 1.8 |
| Drift angle | Y nondimensional force | | |
| | Validation Data | Analysis Result | %Error |
| -4 | $-1.39*10^{-3}$ | $-1.54*10^{-3}$ | 10.9 |
| -2 | $-9.26*10^{-4}$ | $-7.30*10^{-4}$ | 21.2 |
| 2 | $7.01*10^{-4}$ | $7.30*10^{-4}$ | 4.1 |
| 4 | $1.51*10^{-3}$ | $1.54*10^{-3}$ | 2.2 |
| Drift angle | N nondimensional moment | | |
| | Validation Data | Analysis Result | %Error |
| -4 | $-1.10*10^{-3}$ | $-1.05*10^{-3}$ | 4.2 |
| -2 | $-5.22*10^{-4}$ | $-5.28*10^{-4}$ | 1.2 |
| 2 | $5.68*10^{-4}$ | $5.28*10^{-4}$ | 7.1 |
| 4 | $1.11*10^{-3}$ | $1.05*10^{-3}$ | 4.9 |

The validation data of submarine resistance at different depths according to the X-axis are given in Table 6. Validation data is taken from this article (Li, D., et al., 2021). The X force (resistance) obtained by CFD method is nondimensional. The resistance is increasing as the submarne approaches to the free surface, as expected.

**Table 6.** Validation for resistance (Li, D., et al., 2021)

| Depth | Validation Data | Analysis Result | % X difference |
| --- | --- | --- | --- |
| 1.1D | $-2.563*10^{-3}$ | $-2.697*10^{-3}$ | 5.26 |
| 2.2D | $-1.428*10^{-3}$ | $-1.510*10^{-3}$ | 5.79 |
| 3.3D | $-1.125*10^{-3}$ | $-1.205*10^{-3}$ | 7.10 |

Pressure distribution and wave deformation on the free surface obtained from CFD method are also shown for the completeness of the paper in Figures 5 and 6, respectively. It can be seen in the Figure 5 that the positive pressures have been detected in the bow section and fore of the sail and negative pressures in the stern region as expected in depth water. In Figure 6 Kelvin wave pattern has been obtained by CFD method. It can be noted that CFD method is modelling the physical problem properly.
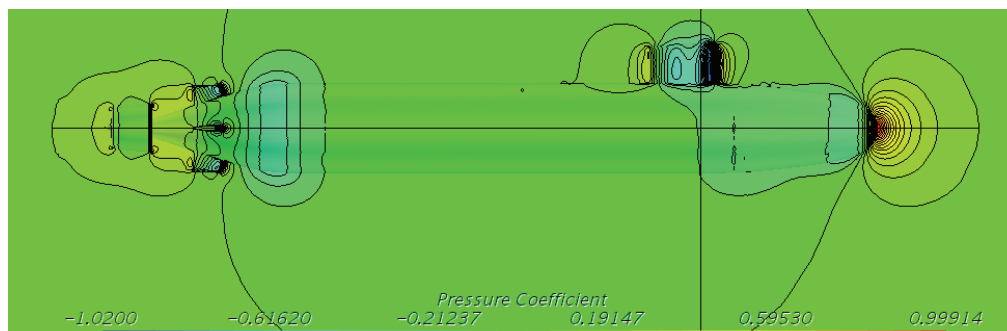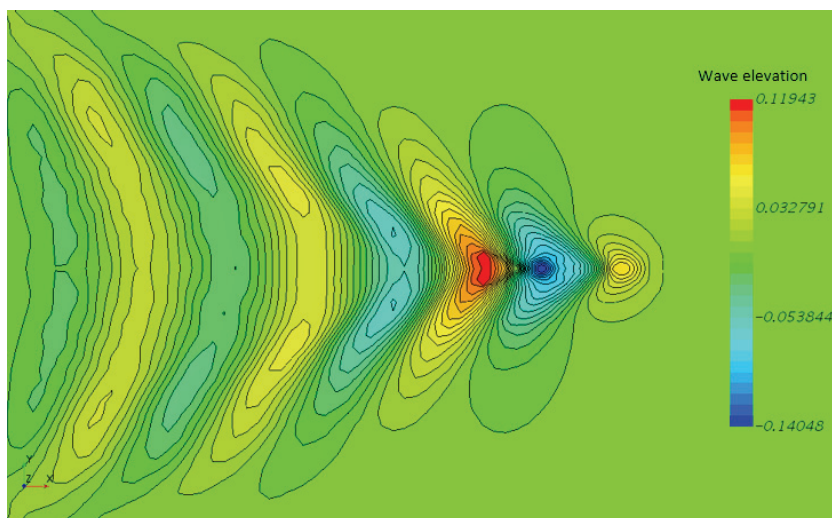


**Figure 5.** Pressure distribution at deep water

**Figure 6.** Kelvin wave pattern at 1.1D

## 4. Cases

The necessary equations for the static drift tests (pure yaw cases) and the determination of hydrodynamic derivatives are given here. Static drift tests are a form of non-accelerated test based on the wall boundary condition. It is initiated with a drag angle. Only forward and lateral translation velocities occur in static drift tests. This test which is free from angular yaw velocity and acceleration, is also free from lateral translational acceleration. The values of the velocities and accelerations of the static drift analyzes are defined in Table 7 according to the submarine coordinates (Yoon, H., 2009).

**Table 7.** Velocities and accelerations in static drift cases (Yoon, H., 2009)

| Motion | Static drift |
|--------|--------------|
| $u$ | $U_c \cos \beta$ |
| $\dot{u}$ | 0 |
| $v$ | $U_c \sin \beta$ |
| $\dot{v}$ | 0 |
| $r$ | 0 |
| $\dot{r}$ | 0 |

Cases at different drift angles and different depths were considered for the $X_v$, $Y_v$ and $N_v$ coefficients determined by static drift analysis. The cases performed for the determination of lateral translational hydrodynamic derivatives in static drift experiments are shown in Table 8.

**Table 8.** Cases studied in static drift analysis.

| Depth | Drift angle | Rudder angle |
|-------|-------------|--------------|
| 6.0D | 4, 2, 0, -2, -4 | 0 |
| 1.1D | 4, 2, 0, -2, -4 | 0 |
| 2.2D | 4, 2, 0, -2, -4 | 0 |
| 3.3D | 4, 2, 0, -2, -4 | 0 |

For the determination of the $X_v$, $Y_v$ and $N_v$ equations, the magnitudes of the X, Y forces and N moment are given in equations 4, 5 and 6, respectively. The equations are in linear form. The effect of angular yaw velocity r is not clearly seen in these equations since the r velocity and acceleration terms are zero.

$$X = X_0 + X_v v \tag{4}$$

$$Y = Y_v v \tag{5}$$

$$N = N_v v \tag{6}$$

Another static drift case is to examine the effect of different rudder angles on the analysis results. In the static drift analysis, $X_\delta$, $Y_\delta$ ve $N_\delta$ coefficients were determined at different rudder angles and at different depths. The cases performed to determine the hydrodynamic rudder coefficients are shown in Table 9.

**Table 9.** Cases used for the determination of rudder derivatives

| Depth | Drift angle | Rudder angle |
|-------|-------------|--------------|
| 6.0D  | 0           | -15, -10, -5, 0, 5, 10, 15 |
| 1.1D  | 0           | -15, -10, -5, 0, 5, 10, 15 |
| 2.2D  | 0           | -15, -10, -5, 0, 5, 10, 15 |
| 3.3D  | 0           | -15, -10, -5, 0, 5, 10, 15 |

Cases used in pure yaw analyzes were performed for the determination of Yr ve Nr hydrodynamic derivatives. These analyzes are dynamic and designed to eliminate the lateral translation velocity and lateral translation acceleration. In Table 10, the pure yaw speeds and accelerations of the model are given with respect to ship coordinate system (Yoon, H., 2009).

**Table 10.** Velocities and accelerations in model coordinates in pure yaw analysis (Yoon, H., 2009)

| Motion | Pure yaw |
|--------|----------|
| $u$ | $U_c\sqrt{1 + \varepsilon^2 cos^2 wt}$ |
| $\dot{u}$ | $-U_c w \dfrac{\varepsilon^2 \sin 2wt}{2\sqrt{1 + \varepsilon^2 cos^2 wt}}$ |
| $v$ | $0$ |
| $\dot{v}$ | $0$ |
| $r$ | $\varepsilon w sinwt \dfrac{1}{1 + \varepsilon^2 cos^2 wt}$ |
| $\dot{r}$ | $\varepsilon w^2 coswt \dfrac{1 + \varepsilon^2(1 + sin^2 wt)}{(1 + \varepsilon^2 cos^2 wt)^2}$ |

The instantaneous angular yaw velocity and angular yaw acceleration in pure yaw analysis of dynamic tests can be defined as in equations 7 and 8, as follows:

$$r = r_{max} sinwt \tag{7}$$

$$\dot{r} = \dot{r}_{max} coswt \tag{8}$$

According to the yaw angular velocity and yaw angular acceleration, the hydrodynamic derivatives to be determined for the Y force and the N moment obtained in the analyzes are Yr and Nr, and additional added masses will also affect the results since the acceleration term is not zero. Hydrodynamic equations of force and moment Y and N are given in equations 9 and 10 as:

$$Y = Y_{\dot{r}}\dot{r} + Y_r r \tag{9}$$

$$N = N_{\dot{r}}\dot{r} + N_r r \tag{10}$$

Forces can also be written as Taylor expansions with respect to model frequency. The frequency in the Taylor series expansion corresponds to the angular yaw velocities of 0.04, 0.08, 0.12 and 0.16 determined for the submarine, and the pure yaw has been determined in accordance with the test results in similar studies. Equations of Taylor expansions have been linearized in this study and higher order terms hare been neglected. Linearized Taylor expansion equations are given in equations 11 and 12 (Yoon, H., 2009) as follows:

$$Y = Y_{c1}coswt + Y_{s1}sinwt \tag{11}$$

$$N = N_{c1}coswt + N_{s1}sinwt \tag{12}$$

The physical equivalents of Taylor expansion coefficients in the equations are given in equations 13-16. Derivative terms used here with sine represent hydrodynamic derivatives (Yr and Nr), derivatives represent by cosine added mass (Yoon, H., 2009).

$$Y_{s1} = Y_r r_{max} \tag{13}$$

$$Y_{c1} = Y_{\dot{r}}\dot{r}_{max} \tag{14}$$

$$N_{s1} = N_r r_{max} \tag{15}$$

$$N_{c1} = N_{\dot{r}}\dot{r}_{max} \tag{16}$$

If a curve as in equation 2 is derived for the Y force and N moment from multiple run method, the relevant coefficients can be obtained (Yoon, H., 2009):

$$y = Ax, \ y = Y, N, \ x = r_{max}, \ Y_r, N_r = A \qquad (17)$$

The cases to be used for the hydrodynamic derivatives (Yr ve Nr) of pure yaw analyzes are given in Table 11.

**Table 11.** Cases for pure yaw derivatives

| Depth | Angular yaw velocities | Rudder angle |
|-------|-----------------------|--------------|
| 6.0D | 0.04, 0.08, 0.12, 0.16 | 0 |
| 1.1D | 0.04, 0.08, 0.12, 0.16 | 0 |
| 2.2D | 0.04, 0.08, 0.12, 0.16 | 0 |
| 3.3D | 0.04, 0.08, 0.12, 0.16 | 0 |

## 5. Hydrodynamics Derivatives

The lateral translation in Yv and Nv derivatives was created with the first order curves according to v velocity, in Yr and Nr derivatives according to yaw angular velocity, and in Xδ, Yδ and Nδ coefficients according to rudder angle. Only in the Xδ derivative, a second-order curve is used due to the force distribution. Dimensionless coefficient curves varying with depth are shown with in Figure 7. As a result, for the nine derivative values given in the graph, the curves of those values were determined and the numerical coefficients were obtained from the first-order slope of the curves. The coefficients change with depths. As a result of this study, the nine linear derivatives was calculated according to four different depths and thirty-six derivatives were determined.
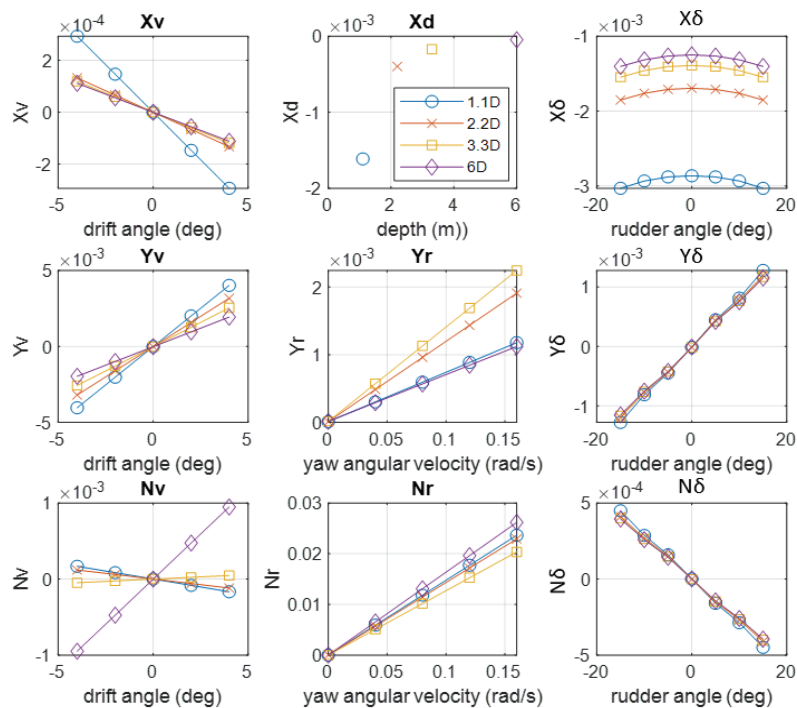


**Figure 7.** Change in nondimensional hydrodynamic derivatives versus depth

Different values were found for nine derivatives at different depths. Curves of each derivative at differet depths have been generated and given. The coefficients are given as nondimensional.  It can be seen from this figure that as the depth increases, many coefficients change, as shown in Figure 8. The physical meaning of this is that free surface affects significantly the submarine at different depths.

In order to produce hydrodynamic derivative curves for the submarine, the depth where the submarine is not affected by the free water surface is defined as deep water. If the depth Froude number is less than 0.7, it is assumed as deep water (Dogrul A., 2019). In addition, Hoerner gave the wave resistance change limit as 5D in his book (Hoerner, S. F., 1965). In this study, the aforementioned deep water depth was chosen as 6D as in the literature (Efremov, D. V., & Milanov, E. M., 2019) and the depth Froude number was 0.61. DSM Deep water analyzes and resistance analyzes at 6D depth were compared and the difference was determined as 3%, and the 3% resistance difference corresponds to the sum of X0 and Xd hydrodynamic derivatives at 6D depth.
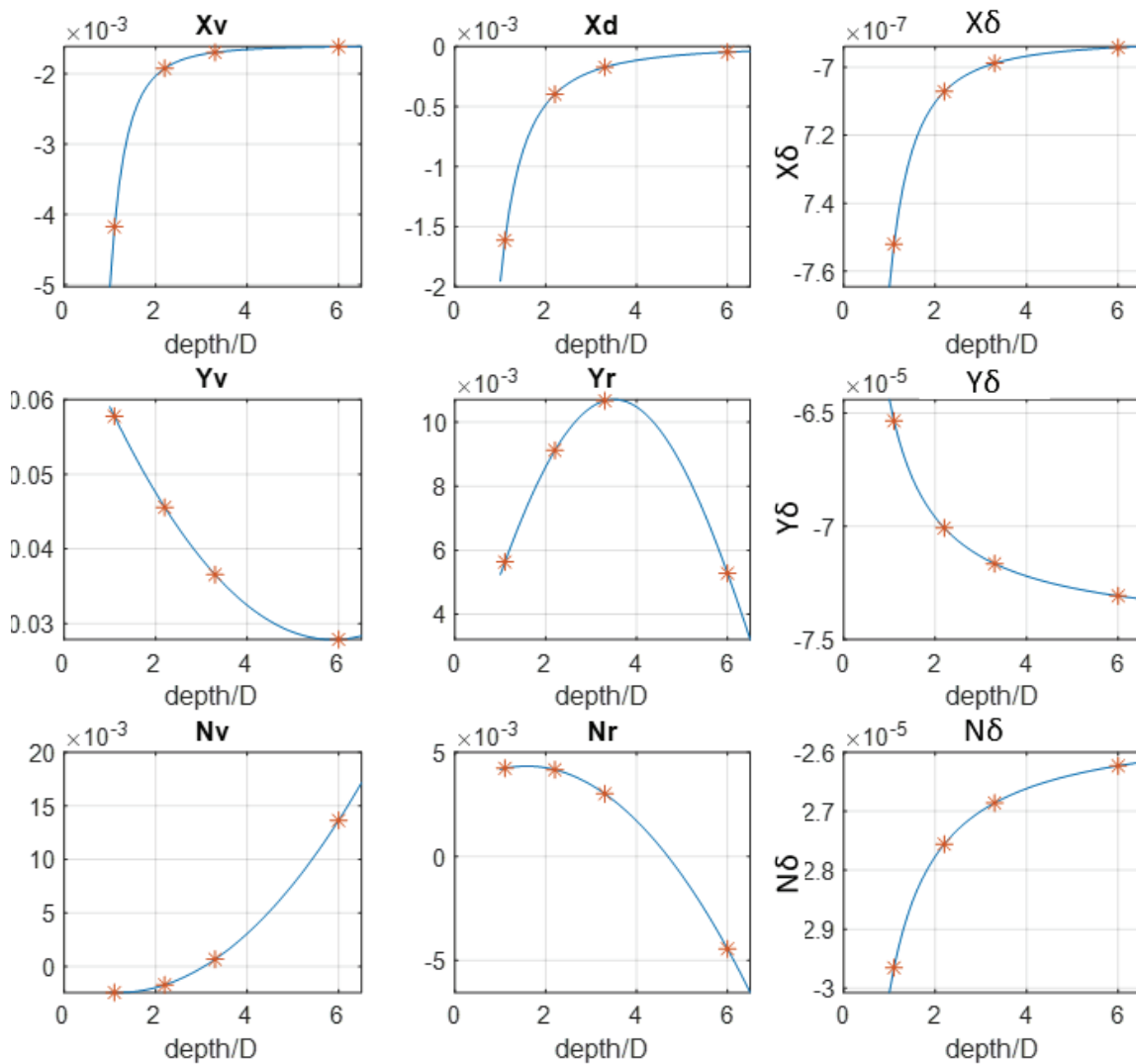


**Figure 8.** Change in hydrodynamic derivatives versus depth

The curves were derived from the coefficients obtained according to the depths and their equations are given below (Equations 18 to 27). With these formulas, the behavior of intermediate values without

computational fluid dynamics studies can be calculated. Δ in the equations represents the depth distance from the free water surface in meters.

$$X0 = -1.25 * 10^{-3} \tag{18}$$

$$Xv = -4.50 * 10^{-4} * \Delta^{-3} - 1.6 * 10^{-3} \tag{19}$$

$$Xd = -5.06 * 10^{-4} * \Delta^{-2} + 8.22 * 10^{-6} \tag{20}$$

$$X\delta = -1.87 * 10^{-8} * \Delta^{-2} - 6.92 * 10^{-7} \tag{21}$$

$$Yv = -5.07 * 10^{-3} * \Delta^{2} + 3.03 * 10^{-2} * \Delta - 7.31 * 10^{-2} \tag{22}$$

$$Yr = -1.07 * 10^{-2} * \sin(0.83 * \Delta + 0.89) \tag{23}$$

$$Y\delta = 5.28 * 10^{-6} * \Delta^{-1} - 7.48 * 10^{-5} \tag{24}$$

$$Nv = -2.68 * 10^{-3} * \Delta^{2} + 3.22 * 10^{-3} * \Delta + 1.46 * 10^{-3} \tag{25}$$

$$Nr = 1.74 * 10^{-3} * \Delta^{2} - 2.80 * \Delta - 3.21 * 10^{-3} \tag{26}$$

$$N\delta = -2.34 * 10^{-6} * \Delta^{-1} - 2.55 * 10^{-5} \tag{27}$$

It is known that there are only linear derivatives in the horizontal stability formula. Using linear coefficients, submarine horizontal stability index is calculated as follows equation 28 and $x'_G m'$ The $x'_G m'$ term is given as -0.127*10-4 (Roddy, 1990).

$$G_h = 1 - N'_v \frac{(Y'_r - m')}{[Y'_v(N'_r - x'_G m')]} \tag{28}$$

According to the literature, if the horizontal stability value is between 0 and 1, the system is stable, if it is greater than 1, the system is overstable, and if it is less than 0, the system is unstable. (Roddy, 1990), indicating that the DSM is actually a model with horizontal stability in its near-surface course. Accordingly, the DSM model is horizontally stable in the three-degree-of-freedom system when traveling near the surface. The horizontal stability-depth graph of the DSM model is shown below. The reason why the horizontal stability behavior is not linear with respect to depth is that the linear derivatives do not show linear behavior with respect to depth. Since hydrodynamic derivatives are exposed to different free surface effects depending on the depth and free surface is nonlinear in nature, they do not show a linear behavior (Efremov and Milanov, 2019). The point with yellow star indicates the extremely stable transition depth and the point with red star indicates the greatest horizontal stability that the submarine had, as shown in Figure 9.

Note that the horizontal stability number of DSM is greater than zero for lower depths of 4.6D, and it takes a value greater than 1 for depths between 3.1D and 4.6D (Figure 9). Therefore, DSM has horizontal stability for up to depths of 4.6D depth, even an extreme stable horizontal stability between 3.1D and 4.6D of depths. Below 4.6D of depth, it does not have any horizontal stability.
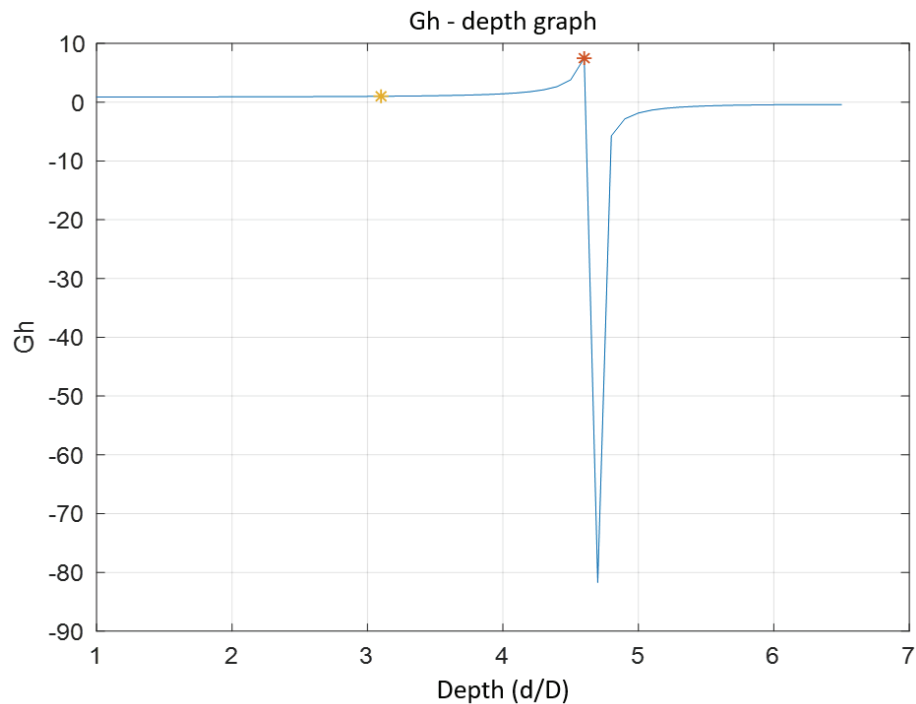
**Figure 9.** Gh values versus depth ratio

## 6. Conclusion

The hydrodynamic derivatives of DARPA Submarine moving at different depths were computed and the horizontal stability was investigated. Mesh independence studies and validation were carried out for the designed model. For the submarine model, CFD analyzes were performed according to the depth values selected from the literature (1.1D, 2.2D, 3.3D and 6D depths) and curve fitting was applied to the values obtained for the intermediate depths. Three degrees of freedom linear system was designed and solved numerically to provide the horizontal stability equation in the submarine model. It has been found that the submarine model has different coefficients versus varying depths and different horizontal stability.

It was found that DSM does not have a horizontal stability in deep water. It is confirmed by the studies given in the literature. But the submarine for shallower depths (up to 4.6D depth) has horizontal stability.

## References

Amiri, M. M., Sphaier, S. H., Vitola, M. A., & Esperança, P. T. (2019). URANS investigation of the interaction between the free surface and a shallowly submerged underwater vehicle at steady drift. *Applied Ocean Research*, *84*, 192-205.

Ashok, A., & Smits, A. J. (2013). The turbulent wake of a submarine model in pitch and yaw. In *Eighth International Symposium on Turbulence and Shear Flow Phenomena*. Begel House Inc.

Duman, S., & Bal, S. (2019). A quick-responding technique for parameters of turning maneuver. *Ocean Engineering*, *179*, 189-201.

Duman, S., & Bal, S. (2021). Prediction of the acceleration and stopping manoeuvres of a bare hull surface combatant by closed-form solutions and CFD. *Ocean Engineering*, *235*, 109428.

Efremov, D. V., & Milanov, E. M. (2019). Hydrodynamics of DARPA SUBOFF submarine at shallowly immersion conditions. *TransNav: International Journal on Marine Navigation and Safety of Sea Transportation*, *13*(2).

Hoerner, S. F. (1965). Fluid-dynamic drag. *Hoerner fluid dynamics*.

Inoue, S., Hirano, M., & Kijima, K. (1981). Hydrodynamic derivatives on ship manoeuvring. *International Shipbuilding Progress*, *28*(321), 112-125.

ITTC, S. (2008). Final Report and Recommendation to the 25th ITTC. *Proceedings of the 25th ITTC. The Seakeeping Committee*.

Kırıkbaş, O., Kınacı, Ö. K., & Bal, S.,. Sualtı Araçlarının Manevra Karakteristiklerinin Değerlendirilmesi-I: Manevra Analizlerinde Kullanılan Yaklaşımlar. *Gemi ve Deniz Teknolojisi*, (219), 6-58.

Kırıkbaş, O., Bal, S., & Baykal, M. A. (2021). Comparison Of The Rules Of Classification Societies (IACS Members) In The Area Of Submersible Maneuvering. *Avrupa Bilim ve Teknoloji Dergisi*, (28), 178-183.

Kırıkbaş, O., Kınacı, Ö. K., & Bal, S., Su Altı Araçlarının Manevra Karakteristiklerinin Değerlendirilmesi-II: Akışkan Sınırlarının Etkileri. *Gemi ve Deniz Teknolojisi*, (220), 135-174.

Liu, Y., Li, Y., & Shang, D. (2019). The hydrodynamic noise suppression of a scaled submarine model by leading-edge serrations. *Journal of Marine Science and Engineering*, *7*(3), 68.

Li, D., Yang, Q., Zhai, L., Wang, Z., & He, C. L. (2021). Numerical investigation on the wave interferences of submerged bodies operating near the free surface. *International Journal of Naval Architecture and Ocean Engineering*, *13*, 65-74.

Racine, B., & Paterson, E. (2005, June). CFD-based method for simulation of marine-vehicle maneuvering. In *35th AIAA Fluid Dynamics Conference and Exhibit* (p. 4904).

Ray, A., Singh, S. N., & Seshadri, V. (2009, January). Evaluation of linear and nonlinear hydrodynamic coefficients of underwater vehicles using CFD. In *International Conference on Offshore Mechanics and Arctic Engineering* (Vol. 43444, pp. 257-265).

Roddy, R. F. (1990). *Investigation of the stability and control characteristics of several configurations of the DARPA SUBOFF model (DTRC Model 5470) from captive-model experiments*. David Taylor Research Center Bethesda MD Ship Hydromechanics Dept.

Sakaki, A., & Kerdabadi, M. S. (2020). Experimental and numerical determination of the hydrodynamic coefficients of an autonomous underwater vehicle. *Zeszyty Naukowe Akademii Morskiej w Szczecinie*.

Sezen, S., Dogrul, A., Delen, C., & Bal, S. (2018). Investigation of self-propulsion of DARPA Suboff by RANS method. *Ocean Engineering*, *150*, 258-271.

Yoon, Hyunse. "Phase-averaged stereo-PIV flow field and force/moment/motion measurements for surface combatant in PMM maneuvers." PhD (Doctor of Philosophy) thesis, University of Iowa, 2009. https://doi.org/10.17077/etd.jgq7s29l